Improving acoustic determinations of the Boltzmann constant with mass spectrometer measurements of the molar mass of argon



2015 Metrologia 52 S394

(http://iopscience.iop.org/0026-1394/52/5/S394)

IOP Publishing | Bureau International des Poids et Mesures Metrologia

Metrologia **52** (2015) S394–S409 doi:10.1088/0026-1394/52/5/S394

# Improving acoustic determinations of the Boltzmann constant with mass spectrometer measurements of the molar mass of argon

**Inseok Yang[1], Laurent Pitre[2], Michael R Moldover[3], Jintao Zhang[4], Xiaojuan Feng[4] and Jin Seog Kim[1]**

[1] Korea Research Institute of Standards and Science, Daejeon, 34113, Korea
[2] Laboratorie Commun de Metrologie LNE-Cnam, 61 rue du Landy, 93210 La Plaine, France
[3] Sensor Science Division, National Institute of Standards and Technology, Gaithersburg, MD 20899, USA
[4] National Institute of Metrology, Beijing 100013, People's Republic of China

E-mail: iyang@kriss.re.kr

Received 20 April 2015, revised 24 July 2015
Accepted for publication 14 August 2015
Published 30 September 2015


**Abstract**

We determined accurate values of *ratios* among the average molar masses $M_{Ar}$ of 9 argon samples using two completely-independent techniques: (1) mass spectrometry and (2) measured ratios of acoustic resonance frequencies. The two techniques yielded mutually consistent ratios (RMS deviation of $0.16 \times 10^{-6}\, M_{Ar}$ from the expected correlation) for the 9 samples of highly-purified, commercially-purchased argon with values of $M_{Ar}$ spanning a range of $2 \times 10^{-6}\, M_{Ar}$. Among the 9 argon samples, two were traceable to recent, accurate, argon-based measurements of the Boltzmann constant $k_B$ using primary acoustic gas thermometers (AGT). Additionally we determined our absolute values of $M_{Ar}$ traceable to two, completely-independent, isotopic-reference standards; one standard was prepared gravimetrically at KRISS in 2006; the other standard was isotopically-enriched $^{40}$Ar that was used during NIST's 1988 measurement of $k_B$ and was sent to NIM for this research. The *absolute* values of $M_{Ar}$ determined using the KRISS standard have the relative standard uncertainty $u_r(M_{Ar}) = 0.70 \times 10^{-6}$ (Uncertainties here are one standard uncertainty.); they agree with values of $M_{Ar}$ determined at NIM using an AGT within the uncertainty of the comparison $u_r(M_{Ar}) = 0.93 \times 10^{-6}$. If our measurements of $M_{Ar}$ are accepted, the difference between two, recent, argon-based, AGT measurements of $k_B$ decreases from $(2.77 \pm 1.43) \times 10^{-6}\, k_B$ to $(0.16 \pm 1.28) \times 10^{-6}\, k_B$. This decrease enables the calculation of a *meaningful*, weighted average value of $k_B$ with a uncertainty $u_r(k_B) \approx 0.6 \times 10^{-6}$.

Keywords: Boltzmann constant, molar mass of argon, mass spectrometer, argon isotope, acoustic gas thermometer

(Some figures may appear in colour only in the online journal)

## 1. Introduction

Today, the unit of the thermodynamic temperature, the kelvin, is based on a defined value of the temperature of the triple point of water: $T_{TPW} = 273.16$ K, exactly. In November 2014, the General Conference on Weights and Measures adopted a resolution planning to replace the present definition of the kelvin in the year 2018 with a new definition based on a defined value of the Boltzmann constant $k_B$ [1]. To prepare for this new definition, an international effort using diverse

 

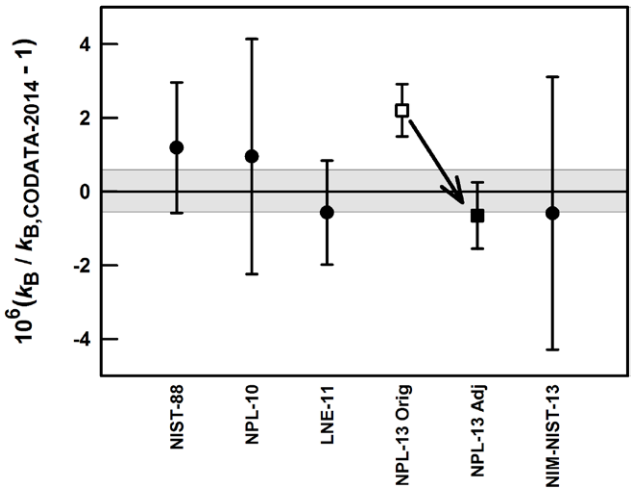


**Figure 1.** Five argon-based acoustic measurements of $k_B$ are compared with the CODATA-2014 value and its uncertainty (shaded band). The value of NPL-13 determination of $k_B$ is adjusted largely due to the new determination of $M_{Ar}$ in the work (adjustment of −2.73 ppm), removing its inconsistency with LNE-11. The plotted values (including NPL-13) also include small adjustments (<0.2 ppm) from the originally published values that CODATA-2014 made to account for more accurate values of the thermal conductivity of argon and the atomic masses of argon isotopes.

techniques and physical principles is measuring $k_B$ as accurately as possible using the current definition [2]. This effort will result in a 'best' value of $k_B$ that will be incorporated into the new definition. This careful preparation will ensure that any future measurement of $T_{TPW}$ made using the new definition of the kelvin (and possibly new techniques and physical principles) will differ from 273.16 K by no more than a few ppm (1 ppm = one part in $10^6$).

Since 1979, acoustic gas thermometry (AGT) has been the most accurate method for measuring $k_B$ [3]. Absolute AGT determines the thermodynamic temperature $T$ by measuring the zero-pressure limit of the speed of sound $c_0$ in a gas with an accurately-known molar mass $M$ [4]. When an AGT is operated at the temperature $T_{TPW}$, it can be used to determine $k_B$ using the equation

$$k_B = \frac{{c_0}^2 M}{\gamma_0 T_{TPW} N_A} \quad (1)$$

where $\gamma_0$ is ratio of specific heats, which is exactly 5/3 for an ideal monoatomic gas, and $N_A$ is the Avogadro constant, which has an uncertainty less than 5% of the uncertainty of $k_B$ [3, 5].

In 1988, the National Institute of Standards and Technology (NIST) measured $k_B$ with the relative uncertainty $u_r(k_B) = 1.7$ ppm using AGT with argon as the test gas [6]. Until 2006, CODATA's evaluation of $k_B$ gave NIST's 1988 result a dominant weight [3]. Since 2006, several new argon-based AGT determinations of $k_B$ have been published. Figure 1 compares these newer determinations of $k_B$ with the NIST-88 result and with the CODATA-2014 evaluation and its uncertainty[5], as indicted by the shaded band [5]. Each value of $k_B$ is identified by the first author's laboratory and by the year of publication. The references for these $k_B$ determinations are: NPL-10 [7]; LNE-11 [8]; NPL-13 [9]; NIM-NIST-13 [10]: (Here and below, 'NPL' refers to the National Physical Laboratory of Great Britain and 'NIM' refers to the National Institute of Metrology, China).

In this work we used mass spectrometry at Korea Research Institute of Standards and Science (KRISS) and measurements of acoustic frequency-ratios at Laboratorie Commun de Metrologie LNE-Cnam (LNE) to determine accurate values of the average molar mass of argon samples $M_{Ar}$ including argon samples traceable to LNE-11 and NPL-13 determinations of $k_B$. LNE-11 reported a value of $k_B$ with an uncertainty of 1.24 ppm; NPL-13 reported a value of $k_B$ with an uncertainty of 0.71 ppm. However, these values of $k_B$ differed by 2.77 ppm which is more than the sum of their claimed uncertainties 1.95 ppm. If the revised value of $M_{Ar}$ determined in this work is used to adjust the NPL-13 result and the uncertainties of the existing results, their mutual inconsistency is removed (see the arrow in figure 1) and the uncertainties of LNE-11 and NPL-13 results are increased only slightly. After this inconsistency is removed, a *meaningful* weighted average can be computed for the values of $k_B$ in figure 1 that has an uncertainty $u(k_B)$ which is smaller than the inconsistency between the two original publications of LNE-11 and NPL-13. Note: In figure 1, the plotted value 'NPL-13 Adj' includes adjustments of −2.73 ppm (for using the KRISS value of $M_{Ar}$) and −0.19 ppm (for a more accurate value of argon's thermal conductivity, see Supplementary information in [4]) from 'NPL-13 Orig.' Similarly, other values of $k_B$ are the results of small adjustment (<0.2 ppm) for more accurate values of argon's thermal conductivity.

The present work was motivated by three observations: (1) The value of $k_B$ determined by AGT is directly proportional to the molar mass of working gas, (2) LNE-11 and NPL-13 described in detail their extensive efforts to accurately measure $c_0$ at $T_{TPW}$; however, neither LNE-11 nor NPL-13 measured $M_{Ar}$ of their argon samples in their *own* laboratories, and (3) the claimed uncertainties $u(M_{Ar})$ (0.15 ppm in LNE-11; 0.39 ppm in NPL-13) were much smaller than it is normally possible to achieve by mass spectrometry in determining the absolute value of the $M_{Ar}$ of argon (order of 1 ppm). These observations led us to suspect that the discrepancy between the values of $k_B$ resulted from one or more errors in determining $M_{Ar}$.

In this work, we determined $M_{Ar}$ for 15 argon samples including 9 whose $M_{Ar}$ ratios were also determined by AGT. We used Lee *et al*'s gravimetrically-prepared isotope standard [11] and KRISS' mass spectrometer to measure the ratios of the abundances of the isotopes $^{36}$Ar, $^{38}$Ar, and $^{40}$Ar, from which $M_{Ar}$ is calculated using the known atomic weights of the isotopes [12]. We checked the precision of the isotope-ratio determinations by KRISS' mass spectrometer by using rigorous gas-handling procedures and an AGT to measure acoustic resonance frequency-ratios of 9 of the 15 samples at LNE. From the combined measurements, we drew 5 conclusions:

[5] All uncertainties are one standard uncertainty with coverage factor $k = 1$ corresponding to 68% confidence limit.

(1) the 9 samples of commercially-purchased, highly-purified argon had values of $M_{Ar}$ spanning a range of 2 ppm implying that isotopic fractionation occurs during commercial processing;
(2) the ratios among the 9 values of $M_{Ar}$, as determined by mass spectrometry and by acoustic frequency-ratio measurements, are mutually consistent to better than 0.2 ppm as shown in figure 5, below;
(3) if our measurements of $M_{Ar}$ are accepted, the discrepancy between the LNE-11 and NPL-13 values of $k_B$ is completely resolved, as shown in figure 1;
(4) some of mass spectrometry determinations of $M_{Ar}$ made at the Institute for Reference Materials and Measurements (IRMM) and KRISS are mutually inconsistent in complicated ways, as shown in figure 6, below; because of (2), we think that the inconsistency is due to the IRMM measurements;
(5) from a direct measurement of the argon gas that was used to measure NPL-13 value of $k_B$, $[(M_{Ar})_{SUERC}/(M_{Ar})_{KRISS} - 1] = (2.73 \pm 0.72) \times 10^{-6}$ and from an indirect measurement link $[(M_{Ar})_{SUERC}/(M_{Ar})_{KRISS} - 1] = (3.61 \pm 0.72) \times 10^{-6}$; in either cases, the inconsistency between SUERC and KRISS deserves more study (SUERC is the Scottish Universities Environmental Research Centre). We recommend the value $(2.73 \pm 0.72) \times 10^{-6}$ because there are fewer chances for isotopic fractionation in the direct comparison.
We made less-extensive mass spectrometry and acoustic frequency measurements at the Key Laboratory of Petroleum Resource Research, Chinese Academy of Sciences (KLPRR-CAS) and at NIM. These measurements led to the additional conclusion:
(6) the absolute values of $M_{Ar}$ determined at KRISS are consistent with NIST's Ar-40 mass standard, within the uncertainty of the comparisons (0.93 ppm; see figure 8, below).

As a result of this work, there are links among the values of $M_{Ar}$ used in NIST-88, NPL-10, LNE-11, NPL-13, and NIM-NIST-13 measurements of $k_B$.

Here, we list the methods used to determine $M_{Ar}$ for the measurements of $k_B$ displayed in figure 1. The value of $M_{Ar}$ for NIST-88 was based on a $M_{Ar}$-standard of argon enriched in the isotope $^{40}$Ar (denoted as 'NIST Ar-40' in the present work) that had a relative uncertainty $u_r(M_{Ar}) = 0.7$ ppm. In NIST-88, ratios of acoustic resonance frequencies were measured to determine the ratio $[(M_{Ar})_{working\ gas}]/[(M_{Ar})_{NIST\ Ar\text{-}40}]$ with an uncertainty of 0.4 ppm. The values of $M_{Ar}$ for NPL-10 and LNE-11 were determined at IRMM using mass spectrometry based on a gravimetrically-generated isotope reference gas [13]. The value of $M_{Ar}$ for NPL-13 (in the original publication) was determined at SUERC by mass spectrometry using local atmospheric argon as a working standard [9]. SUERC assumed that their atmosphere-derived argon had the same isotopic abundances as the atmosphere-derived argon analyzed by Lee *et al* [11] at KRISS. The value of $M_{Ar}$ for NIM-NIST-13 was determined by KLPRR-CAS using the reference gas traced to the KRISS mass spectrometer measurement for a previous NIM determination of $k_B$ [14]. Therefore, the NPL-13 and NIM-NIST-13 values of $M_{Ar}$ are traceable to the same gravimetric isotope reference gas produced at KRISS for the work of Lee *et al* [11].

We emphasize that the present work makes no assumptions concerning atmospheric argon; therefore, our conclusions (1) through (6) do not depend upon resolving the inconsistency between SUERC and KRISS [conclusion (5)].

While reviewing Lee *et al*'s measurement of $M_{Ar}$ for atmosphere-derived argon, de Podesta *et al* [9] noticed that Lee *et al* had made an error in calculating the relative uncertainty $u_r(M_{Ar,atmosphere})$. To correct the error, de Podesta *et al* reduced $u_r(M_{Ar,atmosphere})$ from 5 ppm to 0.35 ppm. In our work, we used much of the same equipment and standards as Lee *et al* and we used improved procedures that achieved $u_r(M_{Ar}) = 0.70$ ppm for the 15 argon samples. Because of this experience, we believe that de Podesta *et al* were too optimistic when they revised Lee *et al*'s uncertainty down to 0.35 ppm. If they had considered some additional uncertainty contributions which we believe do affect the measurement of Lee *et al*, the overall estimated relative uncertainty would have been close to 0.7 ppm.

## 2. Measurements

### 2.1. Argon gas samples

The present research was initiated by LNE to track down the cause of the discrepancy between LNE-11 and NPL-13 values of $k_B$. The research is collaboration among KRISS, LNE, NIM and NIST and it required the exchange of gas samples among these laboratories and other cooperating laboratories, NPL, NMIJ (National Metrology Institute of Japan) and INRIM (Istituto Nazionale di Ricerca Metrologica, Italy). Mass spectrometry measurements were conducted at KRISS and acoustic frequency ratios were measured some of the samples at LNE and NIM. To avoid the remote possibility that the knowledge of a sample's history could unconsciously influence the measurements, we established procedures to conceal the identities and histories of the gas samples until the mass spectrometry measurements and the acoustic frequency measurements were completed and the results of the measurements were deposited at NIST. Only then, the results and the samples' identities were shared among the authors.

A total of 15 argon samples were measured by the mass spectrometer at KRISS. These samples are linked to the argon gases used for previous $k_B$ determinations and/or linked in a complex manner to each other by acoustic measurements, either in previous work or in this work. Table 1 lists the 15 samples with their Sample IDs that identify their laboratory of origin and, in a 'code', their uses. In parentheses, we indicated the symbol '§' followed by the section in this paper where the measurements in the present work (either by mass spectrometer or AGT) are mainly discussed.

The samples in rows 1 through 5 of table 1 were prepared by NPL and sent to KRISS with two-letter sample codes (AA through EE). Sample NPL AA/1 through NPL DD/4 had been

**Table 1.** Argon samples used in this work and their history and/or links.

| Row | Sample ID | History and/or links | Resonance frequency comparisons | Alternative ID and ref. |
|---|---|---|---|---|
| | | KRISS mass spec., Oct 2014 (§3.1 for rows 1 through 4; §3.2.2 for row 5; §3.3 for row 6) | | |
| 1 | NPL AA/1 | $M_{Ar}$ at IRMM for NPL-10 $k_B$ | | 'NPL Sample 1' in [13] |
| 2 | NPL BB/2 | $M_{Ar}$ at IRMM for NPL-10 $k_B$ | | 'NPL Sample 2' in [13] |
| 3 | NPL CC/3 | $M_{Ar}$ at IRMM | | 'NPL Sample 3' in [13] |
| 4 | NPL DD/4 | $M_{Ar}$ at IRMM | | 'NPL Sample 4' in [13] |
| 5 | NPL EE/Iso5 | $M_{Ar}$ at SUERC for NPL-13 $k_B$ | | 'Isotherm 5' in [9] |
| 6 | NIM Argon-01 | | NIST Ar-40 at NIM (§3.3) | |
| | | KRISS mass spec., Nov, Dec 2014 (§2.5) | | |
| 7 | A-INRIM | | LNE1, Jan 2014 (§2.2) | |
| 8 | B-LNE1[a] | | LNE-11-$k_B$ argon, Mar 2010 (§3.1) | |
| 9 | C-NPL | | LNE1, Jan 2014 (§2.2) | Cyl. 'Ar 6271' in [9] |
| 10 | D-LNE1[a] | | Feb 2014 (§2.2) | |
| 11 | E-LNE2 | | LNE1, Feb 2014 (§2.2) | |
| 12 | F-NMIJ | | LNE1, Aug 2014 (§2.2) | |
| 13 | G-LNE1-d[a] | | LNE1, Sep 2014 (§2.2) | |
| 14 | H-NIM | From the same suppliers cylinder as NIM Argon-01 in row 6 | LNE1, Sep 2014 (§2.2) | |
| 15 | I-LNE1[a] | | Sep 2014 (§2.2) | |

[a] These four samples were from the same supplier's large argon cylinder and are collectively referred as 'LNE1' in this publication. This should not be confused with 'LNE Sample 1' in [13]. 'LNE Sample 1' in [13] was used for the determination of $k_B$ in LNE-11 and is refereed as 'LNE-11-$k_B$' in this publication.

previously analyzed by IRMM [13]. Two of these four NPL samples (NPL AA/1 and NPL BB/2) had been used by NPL to determine the value of $k_B$: NPL-10. Sample NPL EE/Iso5 had been analyzed previously at SUERC and used for 'Isotherm 5'to determine the value of $k_B$: NPL-13.

The sample NIM Argon-01 (row 6 of table 1) was contained in a 6 L cylinder that was sent to KRISS for analysis. The same sample in a similar container was sent to LNE for acoustic frequency measurements. At LNE a fraction of the sample was re-packaged in a 25 $cm^3$ container identified as 'H' (row 14, table 1), and also sent to KRISS. NIM did not share its information about NIM Argon-01 until the mass spectrometer measurements at KRISS were completed (see section 3.3, below).

In rows 7 through 15 of table 1, the Sample IDs have a prefix that is only one letter (A through I). At LNE, one of us (LP) measured the acoustic resonance frequencies of these 9 samples using an AGT. The participating laboratories sent their argon samples to LNE in high-pressure cylinders. Therefore, LNE knew the source and the ownership of each gas; however, LNE was not informed about the history of each gas. LNE measured the acoustic frequency ratios of these gases and then put portions of them into 25 $cm^3$ stainless-steel containers using well-controlled gas-handling protocols. The containers had been prepared for this purpose using carefully controlled cleaning protocols (see section 2.2). These containers were labelled A through I and sent to KRISS for isotopic analysis using mass spectrometry.

Acoustic frequency-ratio measurements link sample B-LNE1 to the argon used for the determination of $k_B$ published in LNE-11 (referred as 'LNE-11-$k_B$'in this publication) [8]. Thus the molar mass of the B-LNE1 sample can be traced to the IRMM isotope measurement on argon used for the LNE-11. The sample C-NPL is 'Ar 6271'in the NPL-13 publication and was linked acoustically at NPL with 'Isotherm 5' gas in the work of NPL-13. Therefore, the molar mass of this C-NPL gas is traceable to the SUERC isotope measurement in the NPL-13. The sample H-NIM was from the supplier's cylinder that is identical to NIM Argon-01 in the table 1.

The four samples B-LNE1, D-LNE1, G-LNE1-d and I-LNE1 were taken from the same supplier's cylinder. This redundancy was invaluable for documenting the long-term stability of LNE's AGT and the effects of modifying the AGT during the summer of 2014 (These samples from the same supplier's cylinder are collectively referred as 'LNE1' in this publication. This should not be confused with 'LNE Sample 1' in [13] that was used for the determination of $k_B$ published in LNE-11, and denoted as 'LNE-11-$k_B$'here). The other samples (A-INRIM, E-LNE2 and F-NMIJ) have not, to our knowledge, been previously studied, either by mass spectrometry or AGT.

### *2.2. Acoustic resonance frequency measurements at LNE*

Figure 2 is a schematic diagram of the apparatus that was used at LNE to measure acoustic frequency ratios of the 9 argon samples discussed in this paper. The heart of the apparatus is a 3 liter, quasi-spherical, cavity that was used as an acoustic resonator while argon flowed through it. While each gas sample flowed through the cavity, we measured the resonance frequency $f_{(0,8)}$ of the (0,8) mode. (To identify the acoustic and microwave modes, we use the notation of [4]). The ratios of the measured values of $f_{(0,8)}$ determined the ratios of the speeds of sound among the 9 argon samples. In addition to

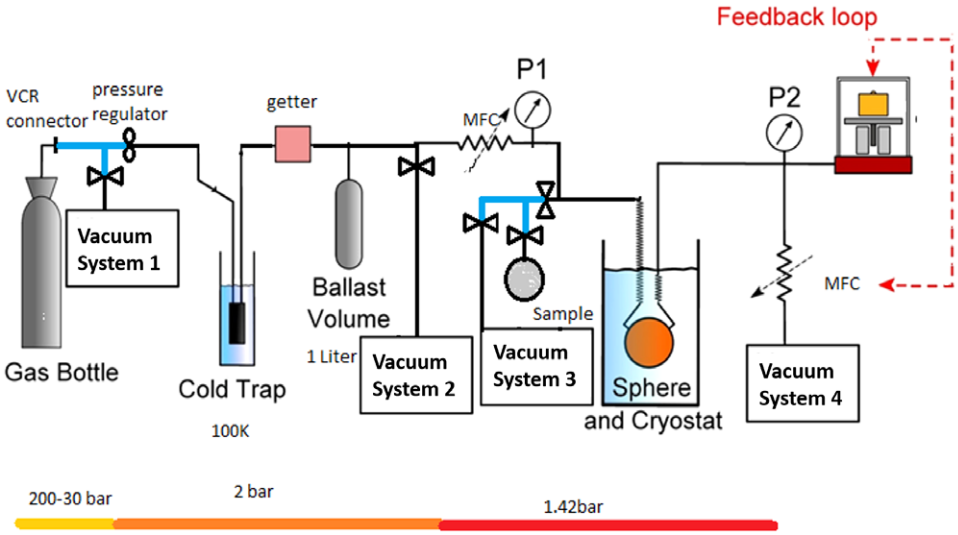


**Figure 2.** Schematic diagram of the gas handling system for the frequency measurements at LNE. P1 and P2 are the pressures measured just upstream and downstream of the cryostat. 'MFC' is a mass flow controller.

the acoustic resonator, the apparatus incorporates systems that: (1) flush the resonator with chemically purified argon, (2) regulate the argon flow through the resonator, (3) regulate and measure the argon pressure inside the resonator, and (4) regulate and measure the temperature of the resonator.

In order to minimize the uncertainty of the comparisons, each gas sample was handled in the same way and each value of $f_{(0,8)}$ was measured within narrow ranges of the temperature $T = (273.160 \pm 0.010)$ K, pressure $p = (142 \pm 0.02)$ kPa, and volume flow rate $\dot{V} = (1.11 \pm 0.02) \times 10^{-2}$ cm$^3 \cdot$ s$^{-1}$ (We estimated $\dot{V}$ at $T = 273.16$ K and $p = 142$ kPa). We then corrected the individual values of $f_{(0,8)}$ to identical values of $P$, and $T$ with precisions of 0.02 mK and 2 Pa. Within the measurement range of $\dot{V}$, the values of $f_{(0,8)}$ were independent of $\dot{V}$. After these corrections, the accuracy of the frequency ratios depended on the quality of the purification and the repeatability of the temperature, pressure, and flow control systems. However, the comparisons are essentially independent of the accuracy of the temperature, pressure, and flow-control systems because any errors in these systems cancel out of frequency ratios measured in narrow frequency ranges. During the acoustic measurements, the resonance frequencies $f_{\mathrm{TE1,3,x}}$ of the microwave triplet TE1,3,x mode were monitored. These microwave frequencies were not used to determine the speed-of-sound ratios. However, they were monitored to detect problems in the apparatus such as an instability in the shape and/or volume of the cavity or a change in the refractive index of the gas in the cavity which might be caused by either changes in the gas's density or the gas's purity.

Here, we provide additional details about the systems used to measure frequency ratios. Then, we discuss the measurement protocols.

The pressure in the resonator and in the gas manifold upstream of the resonator was always 142 kPa or higher. If a leak had been present, argon would mainly leak out of the manifold but air leaking into the manifold would be negligible. A pressure balance (i.e. a mass-loaded piston and cylinder) referenced to vacuum was used to measure the pressure in the resonator. The same pressure balance was linked by a feedback loop to the mass flow controller just upstream from 'Vacuum System 4.' This feedback loop stabilized the pressure in the resonator. Because these components were downstream from the resonator, they did not contaminate the test gases.

Five capsule-type standard platinum resistance thermometers (CSPRTs) were mounted on the resonator. We used a resistance bridge (Model F18, manufactured by Automatic Systems Laboratories[6] Limited) to continuously monitor the ratio of the resistance of one CSPRT to the resistance of a standard resistor that was thermostatted within ±5 mK of a fixed temperature near 25 °C. The resistances of the other 4 CSPRTs were measured just before and just after each sample gas was tested. From the relative drifts of the 5 CSPRTs during the 6 week-long measurement interval, we estimate the uncertainty of the temperature measurements was 0.027 mK, relative to an arbitrary reference temperature within 10 mK of 273.16 K.

The measurements of both the acoustic and microwave resonance frequencies were referenced to a rubidium clock (model FS 725 manufactured by Stanford Research Systems[6] Inc.). The manufacturer specified that the clock's drift is less than 5 part in $10^9$ in 20 years. After correction for small drifts in the resonator's temperature, the values of $f_{(0,8)}$ had a relative standard deviation from their mean of $6.2 \times 10^{-8}$.

A measurement cycle began when a new supplier's cylinder (grade 6.0 argon manufactured by Air Liquide[6]) was connected to the manifold. Then, the small part of the manifold that had been exposed to air was evacuated using 'Vacuum System 1' (see figure 2).

[6] In order to describe materials and procedures adequately, it is occasionally necessary to identify commercial products by manufacturer's name or label. In no instance Institutes (KRISS, LNE-Cnam, NIM) of the authors, nor does it imply that the particular product or equipment is necessarily the best available for the purpose does such identification imply endorsement by the authors' National Metrology.

**Table 2.** The resonance frequencies of the acoustic mode (0,8) and their uncertainties for various argon samples. The listed frequencies have been corrected to 273.16 K and 142 kPa. After these corrections, the frequencies in rows 6 through 11 were multiplied by $(1 - 3.25 \times 10^{-6})$ to account for the change in the volume of the AGT.

| Row | Sample | $f_{(0,8)}$ /Hz | $u(f_{(0,8)})$ /Hz |
|---|---|---|---|
| 1 | B-LNE1 | 12 789.833 45 | 0.0010 |
| 2 | A-INRIM | 12 789.841 11 | 0.0008 |
| 3 | C-NPL | 12 789.836 37 | 0.0008 |
| 4 | D-LNE1 | 12 789.833 35 | 0.0008 |
| 5 | E-LNE2 | 12 789.836 72 | 0.0008 |
| 6 | F-NMIJ | 12 789.827 18 | 0.0015 |
| 7 | X-LNE1 | 12 789.833 04 | 0.0014 |
| 8 | G-LNE1-d | 12 789.832 20 | 0.0018 |
| 9 | Y-NIM-d | 12 789.833 88 | 0.0015 |
| 10 | H-NIM | 12 789.834 46 | 0.0016 |
| 11 | I-LNE1 | 12 789.833 76 | 0.0015 |

We set up an argon flow from the new supplier's cylinder through the cold trap at 105 K, the getter (model HP2 manufactured by Valco Instruments Co.[6], Inc.), the flow-rate-setting mass flow controller, the resonator and ending at 'Vacuum System 4.' In this way, the manifold was flushed with argon from the supplier's cylinder.

In a special test, we monitored the frequency $f_{(0,8)}$ as the argon flushed nitrogen out of the manifold. In that test, $f_{(0,8)}$ decreased towards its steady-state value with a time constant of 19 h in the relevant frequency range of $0.6 \times 10^{-6} f_{(0,8)}$ to $0.1 \times 10^{-6} f_{(0,8)}$. With this time constant as a guide, we established the protocol of flushing the manifold with argon from the supplier's cylinder for 3.5 d and then spending 3.5 d measuring $f_{(0,8)}$ while one of the test samples flowed through the resonator. Even when the supplier's cylinder was not changed, we spent 3.5 d flushing before spending 3.5 d making test measurements. This ensured that the apparatus was subjected to the same flushing process prior to each test measurement. It took 6 weeks to measure $f_{(0,8)}$ for the 5 samples B, A, C, D, and E (Extra time was spent measuring the first sample).

In another special test, (rows 7 and 8 in table 2) we attempted to measure the effects of passing the LNE1 gas through the cold trap and getter. The 'dirty' gas (row 8 in table 2), bypassed the getter and the cold trap. We measured the frequency ratio $[f_{(0,8),\text{X-LNE1}}]/[f_{(0,8),\text{G-LNE1-d}}] = 1 + (0.0\,66 \pm 0.178) \times 10^{-6}$. Within the uncertainty of this test, the cold trap and the getter neither increased nor decreased the resonance frequency in the gas LNE1. Similar test with NIM sample showed negligible change in the bypass test [row 9 ('dirty') and row 10 in table 2]. (However, we note that in some of commercial argon gas we used in the past, the getter had detectable effects on the measured resonance frequency.)

After measuring $f_{(0,8)}$ for samples A through E, we disassembled the thermostat and tightened the bolts that joined together the two halves of the resonator, hoping that we could remove spurious acoustic noise that limited the precision of $k_B$ measurement using the resonator. Unfortunately, tightening the bolts did not reduce the noise; however, it reduced the volume of the resonator, as deduced from the microwave resonance frequencies $f_{\text{TE1,3,x}}$. From the increase in $f_{\text{TE1,3,x}}$, we expected $f_{(0,8)}$ to increase by $(2.24 \pm 0.03)$ ppm; however, $f_{(0,8)}$ actually increased by $(3.25 \pm 0.14)$ ppm. (We determined this increase by comparing measurements of $f_{(0,8)}$ made just before and just after tightening the bolts using the argon from the supplier's cylinder LNE1.) The same operations (disassembly of the thermostat, tightening the bolts, and reassembling the thermostat) caused the frequencies of the other radially-symmetric acoustic modes to increase or decrease a few ppm at 142 kPa. However, these increases and decreases were approximately proportional to the pressure. Thus, the 'shell corrections' to $f_{(0,n)}$ changed and the unexpected frequency increase of $(0.81 \pm 0.14)$ ppm applies only to measurements of $f_{(0,8)}$ conducted near 142 kPa and 273.16 K. We speculate that the change of the shell correction was caused by either a change in the mechanical resonances of the soft copper resonator or changes in the frequencies of resonances in the gas inside the pressure vessel surrounding the resonator. Because these frequency changes decreased linearly with pressure, they do not affect measurements of the Boltzmann constant.

We reassembled the thermostat and used the same protocol described above to measure $f_{(0,8)}$ for samples F, G, H, and I. Table 2 lists the frequency measurements made before and after tightening the bolts. The values of $f_{(0,8)}$ for samples in rows 6 through 11 in table 2 were multiplied by the factor $[1 - (3.25 \pm 0.14) \times 10^{-6}]$ as discussed above. Two samples in table 2 (X-LNE1 and Y-NIM-d) were measured in the AGT at LNE but were not collected in a 25 $\text{cm}^3$ container for the isotope analysis.

### 2.3. Mass spectrometer at KRISS

The isotope measurement at KRISS was performed using the mass spectrometer Finnigan[6] MAT 271 (Thermo Electron, Germany). The mass spectrometer was configured in the single-channel mode and used a single Faraday-cup detector to measure the ion current at a specific mass-to-charge ($m/z$) ratio. For high purity argon sample gases, the only relevant ion currents are from the stable isotopes of $^{36}$Ar, $^{38}$Ar and $^{40}$Ar, which we will denote as $I_{36}$, $I_{38}$, and $I_{40}$, respectively. The ion current at specific $m/z$ is proportional to the partial pressure of the isotope. In a first order approximation, the sensitivity of each isotope of Ar is roughly the same, and the molar isotope ratios $R_{38/36}$ ($\equiv ^{38}\text{Ar}/^{36}\text{Ar}$) and $R_{40/36}$ ($\equiv ^{40}\text{Ar}/^{36}\text{Ar}$) can be assumed to be same as the ion current ratio $I_{38/36}$ ($\equiv I_{38}/I_{36}$) and $I_{40/36}$ ($\equiv I_{40}/I_{36}$), respectively.

In our measurement system, the argon gas in a sample cylinder is diluted by several stages of volumetric expansion. Immediately before the gas is admitted into the ion chamber of the mass spectrometer, the gas is stored in a 1.5 L chamber at a pressure below 5 Pa. When the valve between this chamber and the spectrometer is opened at time $t = 0$, the argon starts to diffuse into the spectrometer through micrometer-sized pin-holes; then, the ionized atoms are detected by the Faraday cup. In this so-called 'dynamic mode,' the mole fraction of the heavier isotope increases over time because lighter isotopes diffuse through pin-holes faster than heavier isotopes. For accurate measurement of the isotope ratios, the ion current ratio at $t = 0$ must be deduced. To achieve this, we measured

the ion currents in the sequence $I_{36}$, $I_{38}$, and $I_{40}$ and we repeated the sequence 15 times during the 25 to 30 min beginning at $t = 0$. The resulting time-dependent values of the ion currents were interpolated to determine the time-dependent ion current ratios: $I_{38/36}$ and $I_{40/36}$. Finally, the time-dependent ion-current ratios were extrapolated to $t = 0$ to obtain the ion-current ratios when the argon sample was first admitted into the spectrometer. We assumed that the $t = 0$ ion current ratios were the isotope ratios of the sample.

For a more precise determination of the isotope ratios, the small difference in the sensitivity of the mass spectrometer for different $m/z$ ratios must be taken into account. We calibrated the mass spectrometer for this 'mass discrimination' effect using argon isotope reference gas mixtures that had well-known isotopic abundance ratios.

We used the two isotope reference mixtures, R3 and R2, that Lee *et al* used in 2006 to re-determine the isotope abundance ratios in atmospheric argon [11]. Lee *et al*'s reference R3 was prepared by gravimetrically mixing highly enriched $^{36}$Ar and $^{40}$Ar to obtain the isotope-abundance ratio $R_{40/36} = 330.30 \pm 0.34$. The uncertainty of the $R_{40/36}$ ratio comes mainly from the resolution of the weighing ($10^{-5}$ g) during the gravimetric preparation and from the uncertainties of the concentrations of chemical impurities in the isotope source gases. Lee *et al*'s reference R2 was prepared by gravimetrically mixing highly enriched $^{36}$Ar with chemically pure near-atmospheric argon. The isotope ratio of R2 was $R_{40/36} = 39.596 \pm 0.037$. After the present measurements were finished, we used R2 to check the validity of the isotope ratio of R3 by confirming the measured isotope ratio was near the expected value (see section 4.2 for details). Within the uncertainty of the check, R3 and R2 were consistent.

During this work, we measured the mass discrimination $f_{\mathrm{MD}}$ of the spectrometer monthly by measuring the ion current ratio generated by the known isotope ratio of the reference mixture R3 and using the formula:

$$f_{\mathrm{MD}} = \left( \frac{R_{\,40/36,\,\mathrm{reference}}}{I_{40/36,\,\mathrm{reference}}} - 1 \right) /4, \qquad (2)$$

where the '4' in the denominator is the difference in the atomic number between $^{36}$Ar and $^{40}$Ar. After $f_{\mathrm{MD}}$ is obtained (i.e. after the mass spectrometer is calibrated), we converted the measured ion current ratios to isotopic abundance ratios using:

$$\begin{aligned} R_{38/36} &= (1+2f_{\mathrm{MD}}) \times I_{38/36} \\ R_{40/36} &= (1+4f_{\mathrm{MD}}) \times I_{40/36} \end{aligned} \qquad (3)$$

In equation (3) we assume that the mass discrimination of the spectrometer between $^{38}$Ar and $^{36}$Ar is the same as the mass discrimination between $^{40}$Ar and $^{36}$Ar.

Then, the molar mass of the argon sample is calculated from the two isotope ratios in (3) and known atomic mass $M_{\mathrm{X}}$ of the argon isotope $^{X}$Ar ($X = 36$, 38 or 40) [12]:

$$M_{\mathrm{Ar}} = \frac{M_{36} + R_{38/36}M_{38} + R_{40/36}M_{40}}{1 + R_{38/36} + R_{40/36}}. \qquad (4)$$

The relative uncertainty in the atomic masses are $8 \times 10^{-9}$, $10 \times 10^{-9}$ and $0.1 \times 10^{-9}$ for $M_{36}$, $M_{38}$ and $M_{40}$, respectively [12]. Because the atomic mass ratios are known so accurately and the isotope abundances of $^{36}$Ar and $^{38}$Ar in atmospheric argon are so small, the uncertainties of the atomic masses make negligible contributions to the uncertainty of the molar mass of the argon samples used in this work. For practical purposes, $M_{\mathrm{Ar}}$ of an argon sample and its uncertainty are determined only by the two isotope ratios $R_{38/36}$ and $R_{40/36}$ of the sample and their uncertainties.

### 2.4. Uncertainty of $M_{Ar}$ of KRISS mass spectrometer measurements

From the previous paragraph and equation (4), the uncertainty of $M_{\mathrm{Ar}}$ is essentially determined by the uncertainty of the two isotope ratios, $R_{38/36}$ and $R_{40/36}$. Near the isotope composition of atmospheric argon, which is close to the isotope composition of all of the high-purity argon samples in this work, the sensitivity of $M_{\mathrm{Ar}}$ to the two isotope ratios is:

relative increase in $R_{38/36}$ by 0.1% corresponds to 0.032 ppm decrease in $M_{\mathrm{Ar}}$;
relative increase in $R_{40/36}$ by 0.1% corresponds to 0.364 ppm increase in $M_{\mathrm{Ar}}$ (5)

Figure 3 illustrates the sensitivity of $M_{\mathrm{Ar}}$ to small changes of the isotope ratios. The sloping, dashed lines are lines of constant $M_{\mathrm{Ar}}$ at interval of 0.5 ppm. The solid line that passes close to the center corresponds to $M_{\mathrm{Ar}} = 39.947\,760$ g mol$^{-1}$, which is close to the samples measured in this work. The large shaded ellipse indicates the total (absolute) uncertainty $u(M_{\mathrm{Ar}})$ and the inner ellipse indicates the short-term repeatability of measurements of $M_{\mathrm{Ar}}$. We now describe the uncertainty contributions which influence our estimate of $R_{38/36}$ and $R_{40/36}$.

*2.4.1. Determination of the mass discrimination, $f_{MD}$.* From equation (2), it is clear that $f_{\mathrm{MD}}$ has uncertainty contributions from the uncertainty of the isotope ratio $u(R_{40/36,\,\mathrm{reference}})$ and from the uncertainty of the measured ion current ratio $u(I_{40/36,\,\mathrm{reference}})$ generated by the isotope reference gas R3. The relative uncertainty contributions are $u_{\mathrm{r}}(R_{40/36,\,\mathrm{reference}}) = 0.34/330.30 = 0.103\%$ from [11] and $u_{\mathrm{r}}(I_{40/36,\,\mathrm{reference}}) = 0.029\%$ from our measurements. Upon combining these contributions in quadrature and dividing by 4, we find $u(f_{\mathrm{MD}}) = 0.000\,27$. From (3), the components of $u_{\mathrm{r}}(R_{38/36})$ and $u_{\mathrm{r}}(R_{40/36})$ from $f_{\mathrm{MD}}$ are 2 $u(f_{\mathrm{MD}})$ and 4 $u(f_{\mathrm{MD}})$, respectively.

*2.4.2. Determination of the ion current ratios $I_{38/36}$ and $I_{40/36}$.* We fitted the measured, ion-current ratios by linear functions of time $t$ to obtain the ratios at $t = 0$ from which we determined the isotope ratio $I_{38/36}$ and $I_{40/36}$. From the fitting, the relative uncertainty of the average $t = 0$ intercepts was $u_{\mathrm{r}}(I_{38/36}) = 0.195\%$ and $u_{\mathrm{r}}(I_{40/36}) = 0.029\%$. The value of $u_{\mathrm{r}}(I_{40/36})$ is the same value that was used for $u_{\mathrm{r}}(I_{40/36,\,\mathrm{reference}})$; this is not a coincidence. It occurred because the ratio $R_{40/36}$ =330.30 of the isotope reference gas R3 is close to the ratios ($296 < R_{40/36} < 300$) of the argon samples involved in this work.

**Table 3.** Uncertainty contributions to the measurements of the isotope ratios and $M_{Ar}$.

| | $R_{38/36}$ | $R_{40/36}$ |
|---|---|---|
| Source of uncertainty | Relative uncertainty | Relative uncertainty |
| $u(f_{MD})$ from $R_{40/36,\,reference}$[a] | 0.051% | 0.103% |
| $u(f_{MD})$ from $I_{40/36,\,reference}$ | 0.015% | 0.029% |
| $u$(ion current ratio) of the sample | 0.195% | 0.029% |
| Detection threshold | 0.577% | 0.110% |
| Root sum of squares = $u_r$(isotopic ratios) | 0.612% | 0.156% |
| $u_r(M_{Ar})$ | 0.19 ppm | 0.57 ppm |
| Combined $u_r(M_{Ar})$ | 0.60 ppm[b] | |

[a] This component is the uncertainty of $M_{Ar}$ measurement due to the isotope reference gas. Combining the effect on the isotope ratios of $R_{38/36}$ and $R_{40/36}$, the contribution of this source on $u_r(M_{Ar})$ is 0.38 ppm.

[b] Because of an additional possible uncertainty term in $R_{38/36}$, which will be discussed in detail in section 4.1, the final combined uncertainty of $M_{Ar}$ measurement using the KRISS mass spectrometer is adjusted to 0.70 ppm.

*2.4.3. Detection threshold of the ion currents.* We now estimate the contribution to $u_r(M_{Ar})$ from the mass spectrometer's ion-current-detection threshold of $2.2 \times 10^4$ counts $s^{-1}$. Before argon is admitted into the mass spectrometer, we always check the blank ion current $I_B$ for each isotope to make sure that the spectrometer's software recognizes the absence of these isotopes and that subsequent, non-zero values of the ion currents originate from the sample. For $^{36}Ar$, $^{38}Ar$, and $^{40}Ar$, $I_B$ is always below the threshold. (For $H_2$, $H_2O$, and $N_2$, $I_B$ is normally above the threshold.) The dominant uncertainty in determining the ratio $I_{38/36}$ comes from the measurement of $I_{38}$ ($\approx 2.2 \times 10^6$ counts $s^{-1}$) and the dominant uncertainty in determining the ratio $I_{40/36}$ comes from the measurement of $I_{36}$ ($\approx 1.15 \times 10^7$ counts $s^{-1}$). However, the measurements of $I_{38}$ and $I_{36}$ ion currents include unknown currents that are below the threshold, that is, between 0 counts $s^{-1}$ and $2.2 \times 10^4$ counts $s^{-1}$. We assess this uncertainty contribution using a one-sided rectangular distribution with the half-width $2.2 \times 10^4$ counts $s^{-1}$ and with the standard deviation $2.2 \times 10^4/\sqrt{3}$ counts $s^{-1}$. Therefore, the relative standard deviation from the unknown blank counts for $I_{38}$ is $(2.2 \times 10^4/\sqrt{3})/(2.2 \times 10^6) = 0.577\%$. Similarly, the threshold contribution to $u_r(I_{36}) = (2.2 \times 10^4/\sqrt{3})/(1.15 \times 10^7) = 0.110\%$. These uncertainty estimates depend on the quantity of sample gas in the inlet volume.

*2.4.4. Combined uncertainty and repeatability.* Table 3 summarizes the uncertainty of the isotope ratios and the molar mass measurement in this work. Combining the uncertainty factors stated above, $u_r(R_{38/36}) = 0.612\%$ [which corresponds to $u(R_{38/36}) = 0.0012$] and $u_r(R_{40/36}) = 0.156\%$ [which corresponds to $u(R_{40/36}) = 0.47$]. The contribution to $u_r(M_{Ar})$ from the uncertainty in $R_{38/36}$ is 0.19 ppm and the contribution from the uncertainty in $R_{40/36}$ is 0.57 ppm. Assuming no correlation between the uncertainties of the two ratios, $u_r(M_{Ar}) = 0.60$ ppm. In figure 3, the standard uncertainty of each of the isotope ratios are represented by the boundaries of the large shaded ellipse.

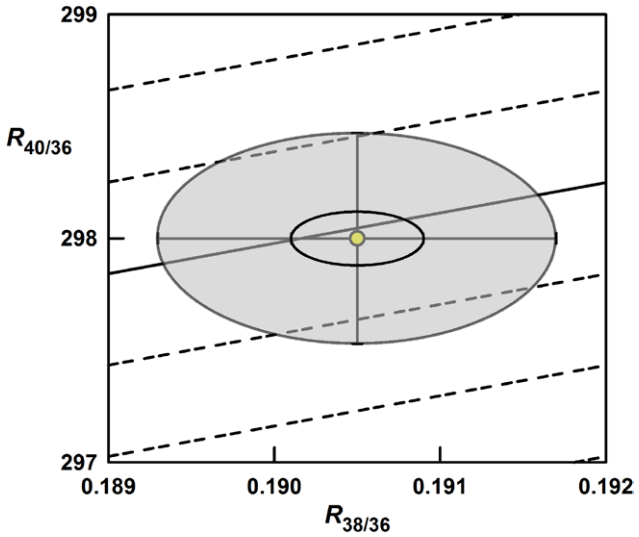


**Figure 3.** The large shaded ellipse spans the absolute uncertainty of isotope-ratio measurements made with the KRISS mass spectrometer. The dashed, sloping lines are lines of constant $M_{Ar}$ at intervals of 0.5 ppm; the solid sloping line represents $M_{Ar} = 39.947\,760\,g\,mol^{-1}$, which is typical in this work. The smaller ellipse at the center indicate the short-term repeatability of the ratio measurements.

Both $R_{38/36}$ and $R_{40/36}$ were calculated using the same value of $f_{MD}$ in equation (3); however, this correction is small; therefore this correlation is not significant. (Also, there is a small correlated uncertainty because both ratios use the same value of $I_{36}$.) For gases with isotopic abundance ratios near those of atmospheric argon, equation (5) shows that the increases of $R_{38/36}$ and $R_{40/36}$ with increasing $f_{MD}$ change $M_{Ar}$ in opposite directions. Therefore, the positive correlation between the uncertainties of the two ratios reduces the uncertainty in $M_{Ar}$ slightly compared to the case where the correlation is ignored.

*2.4.5. Short-term repeatability of the measurement.* A key feature of this work was conducting the isotopic analysis of various argon samples with similar isotopic compositions in a short period of time. Therefore, the measurements of $M_{Ar}$ for the different samples are strongly correlated in time such that the $M_{Ar}$-*ratios* of two samples have a smaller uncertainty than the uncertainty of the absolute values of $M_{Ar}$ for either sample.

One way to assess the uncertainty of $M_{Ar}$-*ratios* of two samples measured during a short period of time is to look carefully at the uncertainty factors in table 3 and estimate the uncertainties that did not change during the two measurements of $M_{Ar}$. However, for example, this approach would not detect changes of $I_B$ below the detection threshold. Therefore, a convincing separation of time-correlated and time-independent uncertainty contributions would be difficult.

Instead we assessed the repeatability of measurements of $M_{Ar}$ from the pooled standard deviation $\sigma_p$ of repeated measurements of the same sample in a short period of time. We determined $\sigma_p$ from 37 measurements of the isotope ratios $R_{38/36}$ and $R_{40/36}$ made on the 15 argon samples listed in table 1. With $\nu = 22$ degrees of freedom, the results for $R_{38/36}$ were $\sigma_p = 0.000\,40$ which is equivalent to $\sigma_p/R_{38/36} = 0.21\%$, and the results for $R_{40/36}$ were $\sigma_p = 0.120$, which is equivalent

**Table 4.** Isotope ratios and molar mass of the samples measured by the KRISS mass spectrometer. The last column shows the molar mass averaged over the two measurements (four measurements only for sample E) in the measurements of November and December, 2014.

| Measurement set | Sample | $R_{38/36}$ | $R_{40/36}$ | $M_{Ar}$ /(g/mol) | $M_{Ar,avg}$ /(g mol$^{-1}$) |
|---|---|---|---|---|---|
| November, 2014 | A-INRIM | 0.190 29 | 297.405 | 39.947 730 | 39.947 728 |
| | B-LNE1 | 0.190 80 | 298.544 | 39.947 782 | 39.947 780 |
| | C-NPL | 0.190 15 | 298.009 | 39.947 761 | 39.947 761 |
| | D-LNE1 | 0.190 98 | 298.131 | 39.947 761 | 39.947 763 |
| | E-LNE2 | 0.190 20 | 297.632 | 39.947 742 | 39.947 748 |
| | F-NMIJ | 0.190 37 | 298.916 | 39.947 803 | 39.947 801 |
| | G-LNE1-d | 0.190 32 | 298.240 | 39.947 771 | 39.947 772 |
| | H-NIM | 0.191 04 | 298.466 | 39.947 777 | 39.947 776 |
| | I-LNE1 | 0.190 67 | 298.386 | 39.947 776 | 39.947 774 |
| December, 2014 | I-LNE1 | 0.190 33 | 298.275 | 39.947 772 | |
| | H-NIM | 0.190 55 | 298.382 | 39.947 776 | |
| | G-LNE1-d | 0.191 03 | 298.410 | 39.947 774 | |
| | F-NMIJ | 0.190 58 | 298.855 | 39.947 799 | |
| | E-LNE 2 | 0.190 70 | 298.056 | 39.947 759 | |
| | D-LNE1 | 0.190 86 | 298.215 | 39.947 766 | |
| | C-NPL | 0.190 56 | 298.087 | 39.947 762 | |
| | B-LNE1 | 0.190 83 | 298.451 | 39.947 778 | |
| | A-INRIM | 0.189 86 | 297.256 | 39.947 726 | |
| | E-LNE 2 | 0.191 47 | 297.827 | 39.947 743 | |
| | E-LNE 2 | 0.190 87 | 297.841 | 39.947 747 | |

to $\sigma_p/R_{40/36} = 0.040\%$. The repeatability of determinations of $M_{Ar}$, as calculated from the repeatability of the measured ratios of the isotopes, was $\sigma_p = 0.16$ ppm. Because the repeatability of the isotope ratios $R_{38/36}$ and $R_{40/36}$ are uncorrelated, the standard uncertainty is represented by an ellipse and shown as the inner ellipse in figure 3.

### 2.5. Measurement of KRISS $M_{Ar}$

KRISS performed the isotope analysis for 9 samples in rows 7 through 15 in table 1 in November 2014 and again, in reverse order, in December 2014. Table 4 lists the isotope ratio measurements ($R_{38/36}$ and $R_{40/36}$) in chronological order. Because the difference between the two measurements on the sample E-LNE2 was at least 3 times larger than the other 8 differences, two additional measurements were performed on this sample at the end of December measurements. The averaged molar mass $M_{Ar,avg}$ was calculated from the two measurements (or four measurements in case of E-LNE2) of the isotope ratios. The mass discrimination factor $f_{MD} = -0.001\,79$ in November and $f_{MD} = -0.001\,72$ in December. Figure 4 shows the isotope ratios averaged over the two sets of measurements for each sample. The ellipse in figure 4 corresponds to the inner ellipse in figure 3; both of these ellipses represent the repeatability of isotope ratio measurements made on the same sample. Below, we discuss the repeatability of the KRISS data for these 9 samples.

The mass spectrometer at KRISS detected a large concentration of hydrogen (80 to 300 μmol mol$^{-1}$) in samples A through E. For samples F through I the hydrogen impurity level was below the detection limit (10 μmol mol$^{-1}$). LNE purchased the 25 cm$^3$ containers for samples F through I after the containers of samples A through E were sent to KRISS in February 2014. The 25 cm$^3$ containers for samples A through E were cleaned by pumping overnight while they were baked at 80 °C. The containers for samples F through I were not baked. It is well known that hydrogen diffuses out of stainless-steel vacuum systems during bakeout; however, vacuum systems are usually baked at much higher temperatures. We believe that the hydrogen in samples A through E was present in the 25 cm$^3$ stainless-steel containers before the argon was transferred into the containers. This is because such high hydrogen impurity levels are inconsistent, by orders of magnitude, with the acoustic measurements listed in table 2. Furthermore, the hydrogen was detected in samples B and D, but not in samples G and I which are all from the sample supplier's cylinder. Therefore, we ignored the hydrogen in our analysis.

The KRISS values of $M_{Ar}$ for the 9 samples span the range 1.73 ppm. As listed in table 2, this range is confirmed by the AGT frequency-ratio measurements at LNE. This range is larger than, or comparable to, the relative uncertainty of the most-accurate, recent $k_B$ determinations. Therefore, argon-based AGT determinations of $k_B$ that hope to achieve uncertainties less than ~3 ppm must determine $M_{Ar}$ for their gas samples. We now know from direct measurements that $M_{Ar}$ varies among high-pressure cylinders of high-purity argon commercially-purchased from diverse vendors around the world.

In section 2.4.5, we assessed the short-term repeatability of the KRISS measurements of $M_{Ar}$ by repeatedly measuring $M_{Ar}$ for a single sample and found $\sigma_p = 0.16$ ppm. Assuming that each of the 9 sample containers is distinct then we calculate $\sigma_p = 0.12$ ppm for the values of $M_{Ar}$ in table 4. Furthermore, we exploit the fact that four samples (B, D, G, and I) originated in the same high-pressure cylinder and, if properly handled, have the same isotopic compositions. In figure 4, these four

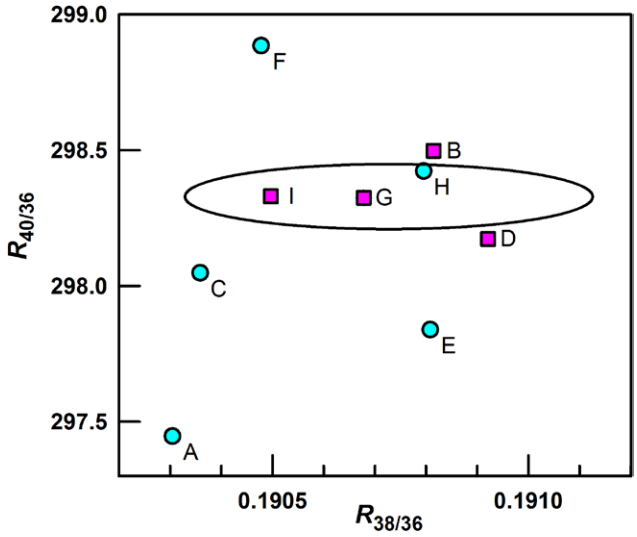


**Figure 4.** KRISS' isotope ratio results for the 9 samples studied at both KRISS and LNE. Squares identify four samples (B, D, G, I) that came from the same supplier's cylinder. The ellipse is centered at the average of *R*40/36 and *R*38/36 for B, D, G, and I; it represents the repeatability of the mass spectrometer measurements.

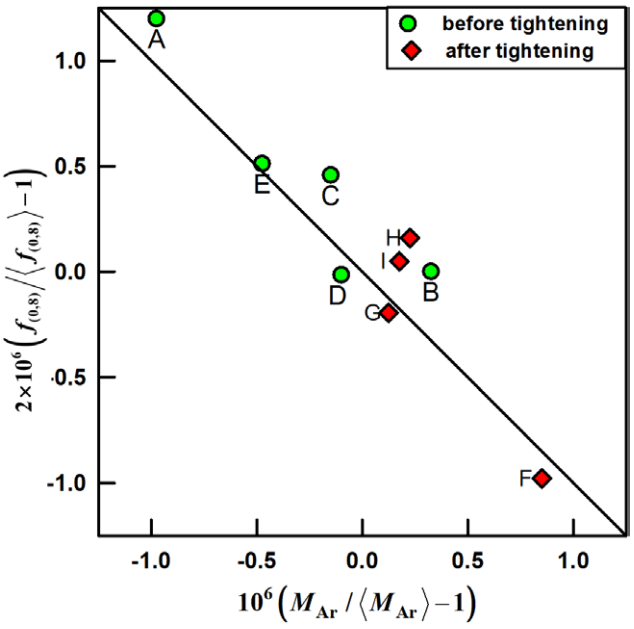


**Figure 5.** Correlation of the KRISS mass spectrometer results with the LNE frequency-ratio results. We plot the deviations of the molar mass (horizontal axis) and the frequency-ratio squared (vertical axis) from their average values among the nine samples studied. The line through the origin with slope −1 was not fitted to the data; the average distance between the data and the line is 0.14 ppm and the RMS distance is 0.16 ppm.

samples are indicated by the same symbols (squares). For these four samples, the relative standard deviation of $M_{Ar}$ from the mean value of $M_{Ar}$ is 0.17 ppm. This measure of repeatability is close to the repeatability determined by repeated measurements of a single sample. (Sample G was not passed through a cold trap and getter; therefore, this result also indicates that the cold trap and getter did not affect isotope ratios of the gas.) The largest difference in $M_{Ar}$ measurement on same sample was 0.43 ppm observed in the sample E-LNE2.

Figure 5 compares the KRISS mass spectrometer measurements and LNE resonance frequency measurements. Considering that the repeatability of the mass spectrometer measurement is 0.16 ppm and the uncertainty in $M_{Ar}$-ratio from frequency measurement is in the order of 0.2 ppm, figure 5 indicates a good agreement between the mass spectrometer and the AGT measurements. The AGT data taken before (circles) and after (diamonds) the bolts were tightened are mutually consistent within their scatter. Recall that the mass spectrometer measurements were performed without knowing the identities of the samples, and that the mass spectrometer and resonance frequency measurements are based on the two completely different physical principles. Thus, figure 5 is strong evidence that both the mass spectrometer results from KRISS and AGT results from LNE do not have significant biases in determining $M_{Ar}$-*ratios* of different samples. We emphasize that figure 5 is based entirely on measurements; there are no fitted parameters. The root mean square distance (measured on the diagonal) between the points and the line is 0.16 ppm.

## 3. Links to the other $M_{Ar}$ measurements

### *3.1. Comparison of the KRISS and IRMM isotope measurements*

The first four samples in table 1 (rows 1 through 4) were previously analyzed by the IRMM mass spectrometer [13]. (see table 1 for identifications in the present paper and in [13]). Both IRMM and KRISS analyzed gas withdrawn from the same four 100 $cm^3$ containers. Therefore, these four samples directly link the mass spectrometers at KRISS and IRMM.

The gas sample B-LNE1 (row 8, table 1) indirectly links KRISS and IRMM. We call this link 'indirect' because it compares the values of $M_{Ar}$ measured at KRISS and IRMM; however, it does not compare the isotopic abundances measured in the two laboratories. This linkage relies on measurements of acoustic frequency ratios using two gas samples: B-LNE1 and the gas used for the LNE-11 measurement of $k_B$ ('LNE-11-$k_B$'). In March 2010, one of us (LP) measured the frequencies of the $f_{(0,4)}$ mode of the 50 mm diameter AGT that was used in LNE-11. The measurement conditions were: $T = 273.32$ K, $p = 100.7$ kPa, and $V = (1.80 \pm 0.02) \times 10^{-2}$ $cm^3 \cdot s^{-1}$. For the LNE-11-$k_B$ argon, the result was: $f_{(0,4),\text{LNE-11-kB}} = (10\ 692.760\ 36 \pm 0.000\ 88)$ Hz; for the B-LNE1 argon the result was $f_{(0,4),\text{B-LNE1}} = (10\ 692.759\ 01 \pm 0.000\ 88)$ Hz. Therefore, we obtain $(M_{\text{B-LNE1}})/(M_{\text{LNE-11- kB}}) = 1 + (0.25 \pm 0.23) \times 10^{-6}$. (Unfortunately, there was not enough LNE-11-$k_B$ gas for acoustic frequency measurements at LNE. Therefore LNE-11-$k_B$ was not included in the measurement campaign in 2014.)

We combine the result from KRISS' mass spectrometer $M_{\text{Ar,B-LNE1}} = (39.947\ 780 \pm 0.000\,024)$ g $mol^{-1}$ (table 4) with the LNE frequency-ratio result to obtain the KRISS-LNE value $M_{\text{Ar,LNE-11-kB}} = (39.947\,770 \pm 0.000\,026)$ g $mol^{-1}$. We compare this KRISS-LNE value with the IRMM value $M_{\text{Ar,LNE-11-kB}} = (39.947\,805 \pm 0.000\,006)$ g $mol^{-1}$ [8, 13] to obtain $[(M_{Ar})_{IRMM}/(M_{Ar})_{KRISS\text{-}LNE} - 1] = (0.88 \pm 0.66) \times 10^{-6}$ for the LNE-11-$k_B$ argon. This indirect comparison does not provide

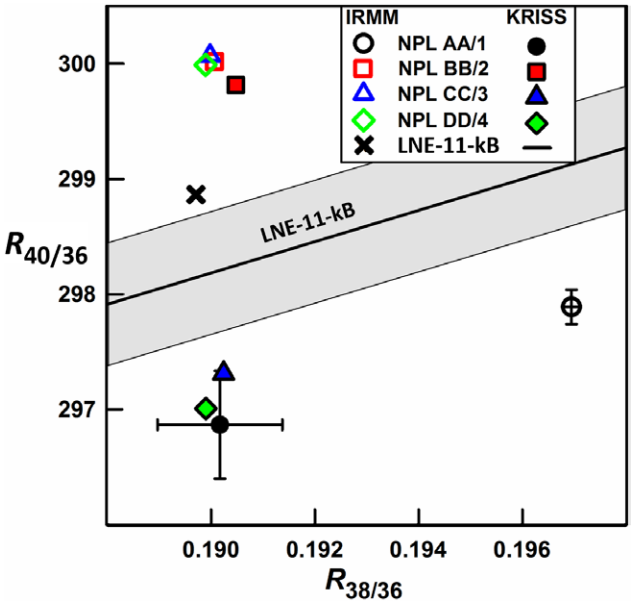


**Figure 6.** Comparison of KRISS (filled symbols) and IRMM (open symbols) isotope analyses on 5 samples.The standard uncertainty claimed by each laboratory is indicated on each data point for NPL AA/1; the uncertainties of the other points are similar for each laboratory. The thick cross (x) represents the IRMM result for LNE-11-$k_B$ argon; the KRISS + LNE result for the same gas is represented by the sloping line with the standard uncertainty indicated as a shaded area.

individual ratios of $R_{38/36}$ and $R_{40/36}$; therefore, we represent it by a line of constant $M_{Ar}$ in the $R_{38/36}$–$R_{40/36}$ plane (figure 6).

Figure 6 compares the isotope measurements of KRISS and IRMM on the first four samples in table 1 (rows 1 through 4) and LNE-11-$k_B$ argon. For the first four samples, the KRISS results are represented with filled symbols (circle, square, triangle, diamond) and the IRMM results are represented by the similarly-shaped symbols without filling. The IRMM measurement of the LNE-11-$k_B$ argon is shown as a thick cross (**x**), and the corresponding KRISS estimate is indicated by the solid sloping line. For clarity, the uncertainty claimed by each laboratory is indicated only for the two circles representing NPL AA/1. Similar uncertainties apply to the other samples from the same laboratories. The uncertainty of the constant-$M_{Ar}$ line for LNE-11-$k_B$ argon estimated by KRISS is indicated by the shaded band surrounding the line. The half-width of this band (0.64 ppm of $M_{Ar}$) is the combination of 0.60 ppm (from the absolute uncertainty of KRISS' mass spectrometer) with 0.23 ppm (the uncertainty of LNE's $M_{Ar}$-ratio measurements by resonance frequencies).

In figure 6, among four pairs of symbols representing the samples that both KRISS and IRMM analyzed directly, only one of these pairs (squares for NPL BB/2) represents mutually consistent results from the two laboratories. The relative difference between the two $M_{Ar}$ measurements was 0.27 ppm. The KRISS and IRMM results for LNE-11-$k_B$ argon are consistent. (If $k = 1$ uncertainty bars were added to the thick cross **x**, they would almost touch the KRISS $k = 1$ uncertainty band.) For LNE-11-$k_B$, the difference between the two values of $M_{Ar}$ was 0.88 ppm, which is only slightly larger than 0.79 ppm, which is the sum of the uncertainty 0.64 ppm of the KRISS + LNE determination of $M_{Ar}$ and 0.15 ppm, which is the claimed uncertainty of IRMM's measurement of $M_{Ar}$.

The KRISS and IRMM results for samples NPL AA/1, NPL CC/3 and NPL DD/4 are inconsistent. The discrepancy in $R_{40/36}$ for NPL CC/3 and NPL DD/4 is 6 times the combined uncertainty of $u(R_{40/36})$ claimed by the two laboratories. The discrepancy in $R_{38/36}$ for NPL AA/1 is 5.8 times the combined uncertainty of $u(R_{38/36})$.

Although the values of $R_{38/36}$ and $R_{40/36}$ for the sample NPL AA/1 from the two laboratories are inconsistent, the values of $M_{Ar}$ from both laboratories differ by only 0.04 ppm. (In figure 6, a line connecting the two circles representing $M_{Ar}$ for NPL AA/1 would be nearly parallel to the constant-$M_{Ar}$ line drawn for the KRISS estimation on the LNE-11-$k_B$.) For the samples NPL CC/3 and NPL DD/4, the fractional difference in the values of $M_{Ar}$ are 3.43 ppm and 3.63 ppm, respectively.

We summarize the contents of figure 6 with the simple statement: the isotope-ratio results from KRISS and IRMM are mutually consistent for only two of the five samples considered.

The known measurements of acoustic frequency ratios cannot determine which, if either, laboratory is correct. The samples NPL AA/1 and NPL BB/2 were used in the AGT determination of $k_B$ in NPL-10 at NPL in the 'fixed' and 'hung' configuration, respectively. The average of the two results was used to determine $k_B$ in NPL-10 [7]. The values of $k_B$ values derived from each configuration were 0.20 ppm and 1.21 ppm higher than CODATA-2014 $k_B$ value, respectively. If we replace the IRMM values of $M_{Ar}$ of NPL AA/1 and NPL BB/2 with the corresponding KRISS values, the $k_B$ values then become 0.16 ppm and 0.94 ppm higher than the CODATA-2014 $k_B$ value, respectively. The differences are all within the uncertainty of the NPL-10 $k_B$. Considering also that the difference between IRMM and KRISS results on $M_{Ar}$ of the LNE-11-$k_B$ argon is 0.88 ppm, the differences in $M_{Ar}$ from IRMM and KRISS on NPL AA/1, NPL BB/2 and LNE-11-$k_B$ argon are not large enough to decisively conclude which sets of measurements are correct. To our knowledge, there are no acoustic results or third-party mass spectrometer measurements that could resolve the inconsistent isotopic analyses of NPL CC/3 and NPL DD/4.

We recall the good agreement between the $M_{Ar}$ determined from KRISS' isotope measurements and the LNE acoustic frequency-ratio measurements (figure 5 and section 2.5). The average distance of the nine measurements from the line of perfect agreement in figure 5 is only 0.14 ppm, and the largest distance is 0.27 ppm. This convinces us that the *relative* results of KRISS's isotope measurements are consistent. We assert that it is statistically very unlikely that out of five measurements of KRISS described in this section, two measurements were inconsistent with the other three measurements by more than 3 ppm. Therefore, we attribute the inconsistency between IRMM and KRISS values of $M_{Ar}$ to inconsistency among the IRMM measurements.

### *3.2. Link to the NPL-13 $k_B$ argon*

*3.2.1. Indirect link via the sample C-NPL.* The identity of sample C-NPL was not shared with either LNE or KRISS until the acoustic and mass spectrometer analyses described in section 2.5 were completed. Only then, C-NPL was identified as being drawn from the cylinder 'Ar 6271,' in the publication of NPL-13 $k_B$ [9]. NPL used its AGT to make a highly-accurate frequency-ratio measurement between 'Ar 6271' and the gas 'isotherm 5' in [9]. (NOTE: However, 'Ar 6271' is not the Ar used in determination of NPL-13 $k_B$, but 'isotherm 5'is.) Therefore, C-NPL links indirectly the KRISS mass spectrometer to the SUERC mass spectrometer analysis of NPL-13 $k_B$ argon through NPL's resonance frequency measurements. The SUERC value of $M_{Ar}$ of the isotherm 5 argon in NPL-13 is 39.947 816 g/mol, with the claimed relative uncertainty $u_r(M_{Ar}) = 0.39$ ppm.

From table 4, KRISS value of $M_{Ar}$ Ar 6271 (sample C-NPL) is 39.947 761 g mol$^{-1}$. From the NPL resonance frequency comparisons, $[(M_{\text{NPL isotherm 5}})/(M_{\text{Ar 6271}}) - 1] = (2.23 \pm 0.03) \times 10^{-6}$. (This could be inferred from figure 7 of [9], and the exact value was taken from private communication with the lead author.) Using this indirect link, the KRISS estimate is $M_{Ar} = 39.947\,672$ g mol$^{-1}$ for the NPL isotherm 5. Therefore, the difference between SUERC's and KRISS' values is $[(M_{Ar})_{SUERC}/(M_{Ar})_{KRISS} - 1] = (3.61 \pm 0.72) \times 10^{-6}$ for the isotherm 5 argon for NPL-13 $k_B$. The uncertainty of the offset is dominated by the uncertainty of KRISS' and SUERC's measurements of $M_{Ar}$ because the uncertainty in the frequency-ratio measurement at NPL that linked between isotherm 5 and Ar 6271 is only 0.03 ppm.

As discussed in section 3.1, the KRISS estimate of $M_{Ar}$ of the LNE-11-$k_B$ argon was smaller than the IRMM value of $M_{Ar}$ of the same sample by 0.88 ppm. Therefore, we can deduce that there is a clear offset between the SUERC $M_{Ar}$ measurement and the IRMM $M_{Ar}$ measurement on the LNE-11-$k_B$ argon. If SUERC and IRMM measured an argon sample in an exactly same condition as SUERC did on NPL-13 $k_B$ argon and IRMM did on LNE-11-$k_B$ argon, respectively, we expect that $[(M_{Ar})_{SUERC}/(M_{Ar})_{IRMM} - 1] = 2.73 \times 10^{-6}$. (Here, $2.73 = 3.61 - 0.88$.) Therefore, we now have evidence that the discrepancy of 2.77 ppm between the LNE-11 $k_B$ and NPL-13 $k_B$ is due to the inconsistency of the measurement of $M_{Ar}$. After fixing this error the discrepancy will be completely resolved, and the two determinations of $k_B$ will agree within their claimed uncertainty.

We note that this finding does not rely on the absolute values of the KRISS $M_{Ar}$. Instead, it relies on three factors: (1) the *internal consistency* of the KRISS $M_{Ar}$ measurements for different samples; (2) internal consistency of the frequency-ratio measurement at LNE; and (3) previous frequency-ratio measurement at NPL [9]. In the present work, factors (1) and (2) are demonstrated by the consistency of the two measurements, as shown in figure 5. Factor (3) was demonstrated in [9] which reported consistent mass spectrometer and frequency-ratio measurements using three argon gases (gases for isotherms 3 and 4; isotherm 5; and isotherms 6 and 7) (see table 2 and figure 7 in [9]).

**Table 5.** The isotope analysis at KRISS on the NPL EE/Iso5.

| Run # | $R_{38/36}$ | $R_{40/36}$ | $M_{Ar}$ /(g mol$^{-1}$) |
|---|---|---|---|
| #1 | 0.189 844 | 296.879 | 39.947 707 |
| #2 | 0.189 821 | 296.874 | 39.947 707 |
| Average | 0.189 833 | 296.876 | 39.947 707 |

*3.2.2. Direct measurement NPL Isotherm 5 argon.* In October 2014, one of the samples that was analyzed by the mass spectrometer at KRISS was from the isotherm 5 argon in NPL-13 [9], listed as NPL EE/Iso5 in table 1 (row 5). The identity of this sample bottle was not shared with KRISS before the final report of the measurement was sent to NPL. Table 5 shows the result of the two measurements on the NPL EE/Iso5 sample as reported to NPL.

For this particular sample, the values of $R_{38/36}$ and $R_{40/38}$ in the two runs of measurements were very close. In our judgement, this is a coincidence that is not representative of the repeatability of the measurements. Therefore, we conservatively assume that the uncertainty of this measurement is comparable to the uncertainty in table 3, $u_r(M_{Ar}) = 0.60$ ppm.

The KRISS measurement showed that $M_{Ar} = 39.947\,707$ g mol$^{-1}$ for the isotherm 5 argon in NPL-13 $k_B$. Because both SUERC and KRISS measured the same sample, we have a direct link between the two measurements which gives the result $[(M_{Ar})_{SUERC}/(M_{Ar})_{KRISS} - 1] = (2.73 \pm 0.72) \times 10^{-6}$ for this sample. If the NPL-13 value of $k_B$ is re-evaluated by replacing the SUERC value of $M_{Ar}$ with the KRISS value of $M_{Ar}$ and if the values of $M_{Ar}$ for other gases used for NPL-13 $k_B$ are adjusted by the same fraction, then the NPL-13 $k_B$ will be decreased by 2.73 ppm. Then, the discrepancy between the LNE-11 and NPL-13 determinations of $k_B$ will be completely resolved. (see figure 1)

We note that the offset of the SUERC measurement relative to the KRISS measurement is 3.61 ppm in the indirect link by the sample C-NPL (section 3.2.1), but 2.73 ppm in the direct link by NPL EE/Iso5. The KRISS $M_{Ar}$ measurement on NPL EE/Iso5 was performed in October 2014, when $f_{MD}$ of the mass spectrometer was +0.000 27. The $M_{Ar}$ measurement at KRISS on the nine samples table 4, including the sample C-NPL, was conducted in November and December 2014, when $f_{MD}$ of the mass spectrometer was −0.001 79 and −0.00 172, respectively. The different values of $f_{MD}$ from the October and November/December calibration indicate that the state of the mass spectrometer was very different during the two sets of measurements. In fact, at the end of October 2014, the inlet volume of the mass spectrometer was opened to replace a valve near the outlet port of the ionization chamber, and the magnet position of the spectrometer was adjusted following the maintenance. Therefore, it is reasonable to expect that the correlation between the two sets of experiments was much weaker than the correlation among the data that was taken in the same month. However, because the mass spectrometer was calibrated after this maintenance using the isotope reference gas R3, the uncertainty assessment on the absolute $M_{Ar}$ measurements as shown in table 3 properly includes the effect of this change.

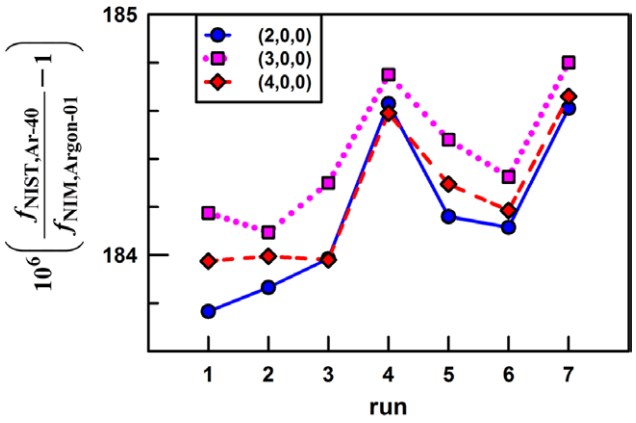


**Figure 7.** Results of frequency-ratio measurements at NIM comparing the two gases NIM Argon-01 and NIST Ar-40. Three acoustic modes were used in each of 7 runs.

The difference between the two sets of measurements (3.61 ppm − 2.73 ppm = 0.88 ppm) is consistent within our estimate of the overall uncertainty. However, the two sets of measurements share a common reference isotope gas R3. Excluding the effect of the reference isotope gas in table 3, the uncertainty is $u_r(M_{Ar}) = 0.47$ ppm. The 0.88 ppm difference between the two experiments that are only correlated by the use of common reference gas is larger than one would hope for, but still consistent within our uncertainty assessment.

### 3.3. Link to NIST Ar-40

A single large cylinder of argon at NIM linked the mass spectrometry at KRISS to acoustic frequency-ratio measurements at both LNE and NIM and also to the gas 'NIST Ar-40' that had been used in the NIST-88 measurement of $k_B$ [6].

In May 2014, about 180 L of argon from the supplier's large cylinder at NIM was transferred to a 6 L cylinder and then shipped to LNE. While acoustic frequency-ratio measurement using this gas was performed at LNE in September 2014, a small fraction of this gas was transferred into a 25 $cm^3$ container that was labelled 'H' during the blind tests (row 14 in table 1). The 25 $cm^3$ container was then shipped to KRISS along with other gas samples for isotopic analysis. As shown in table 4, $M_{Ar}$ of the sample H-NIM measured by the KRISS isotope analysis averaged over two runs of measurements was 39.947 776 g $mol^{-1}$ with the uncertainty $u_r(M_{Ar}) = 0.60$ ppm.

In August 2014, the argon from the same supplier's large cylinder at NIM was transferred to another 6 L cylinder and then shipped to KRISS. In October 2014 this sample (NIM Argon-01, row 6 in table 1) was analyzed using the KRISS mass spectrometer. The result was $R_{38/36} = 0.190\ 71$ and $R_{40/36} = 298.963$. The resulting $M_{Ar}$ of this sample was 39.947 803 g $mol^{-1}$. The uncertainty was $u_r(M_{Ar}) = 0.60$ ppm, which is comparable to the uncertainties in table 3.

In November 2014, two of us (JZ and XF) used a cylindrical (80 mm-long, 80 mm-diameter) primary AGT at NIM to measure ratios of the acoustic resonance frequencies of two gas samples: (1) NIM Argon-01 and (2) NIST Ar-40. At NIM, we used a getter to chemically purify a portion of the NIST Ar-40 that had never been removed from the supplier's cylinder. The cylindrical AGT, the chemical purification, and the methods of measuring acoustic frequencies at NIM are described in the recent NIM-NIST-13 determination of $k_B$ [10].

The resonance-frequency ratios were measured near 300 kPa and 273.16 K. The measurements were repeated in 7 runs during 26 d; each run used three longitudinal acoustic modes denoted (2,0,0), (3,0,0), and (4,0,0). The results from the three modes were mutually consistent; the average standard deviation from the means of the 7 triplets was equivalent to 0.13 ppm of the frequency ratio (see figure 7). The average of all 21 frequency-ratio measurements determined $(M_{NIM,Argon\text{-}01})/(M_{NIST,Ar\text{-}40}) = 1 - (368.55 \pm 0.61) \times 10^{-6}$. Here the uncertainty is the standard deviation of the 21 ratio measurements from their mean. These deviations were dominated by unexpected run-to-run variations as shown in figure 7. It is unlikely that they were caused by imperfections of the temperature and/or pressure control because, as discussed above, such imperfections cancel out of the ratio measurements nearly completely. Feng *et al* report similar run-to-run variations in their measurements of $k_B$ and they speculated that the two resonators that operated in the same pressure vessel were weakly coupled to each other, either electrically or mechanically, and that the coupling was lossy [15]. If so, the measured resonance frequencies were determined, in part, by the coupling, much like the textbook problem of coupled pendula. Feng *et al* speculated that run-to-run variations in the coupling led to unexpected frequency changes.

The average $M_{Ar}$ of NIST Ar-40 was 39.962 517 g $mol^{-1}$, including the effects of Ne, Kr, Xe and $^{38}$Ar. Therefore, $M_{Ar}$ of the NIM Argon-01 was 39.947 788 g $mol^{-1}$ with the fractional uncertainty of 0.93 ppm. This uncertainty is the sum in quadrature of the uncertainty of $M_{Ar}$ of the reference NIST Ar-40 (0.7 ppm) and the uncertainty of the resonance frequency comparisons at NIM (0.61 ppm). Additional details concerning the NIM frequency-ratio measurements using NIST Ar-40 and other argon samples will be published in the future.

Figure 8 displays the values of $M_{Ar}$ discussed in this section for gas samples originating in NIM Argon-01 gas. The KRISS value of $M_{Ar}$ for the NIM Argon-01 gas taken from the 6 L cylinder is 0.37 ppm larger than NIM's frequency-ratio value of $M_{Ar}$. The KRISS value of $M_{Ar}$ for the sample H-NIM (which started as another 6 L cylinder from the same manufacturer's large cylinder and was transported in a 25 $cm^3$ container) is 0.30 ppm smaller than NIM's frequency-ratio value of $M_{Ar}$.

In figure 8, the difference between these two KRISS values of $M_{Ar}$ is 0.67 ppm, which is comparable to the uncertainty of the absolute value of $M_{Ar}$; however, the 0.67 ppm difference is 4 times larger than the repeatability of the KRISS measurements of $M_{Ar}$. The 0.67 ppm difference is consistent in both direction and magnitude with our finding discussed in section 3.2.2 that the calibration of the mass spectrometer seemed to undergo a systematic shift between the October 2014 measurements and the November/December 2014 measurements such that the October measurements resulted in larger values of $M_{Ar}$ than November/December measurements. However, in this case again, the offset was within the uncertainty claim

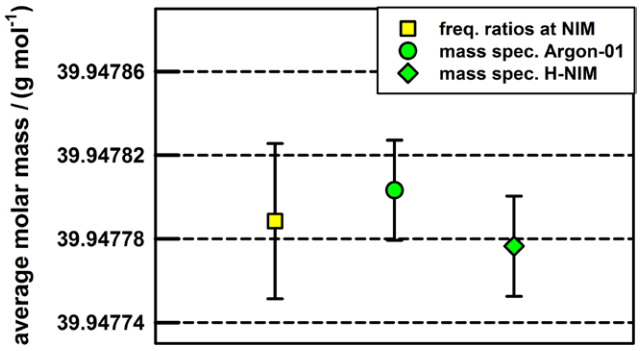


**Figure 8.** The molar mass of the NIM Argon-01 sample determined by the resonance-frequency comparisons at NIM (square) and by mass spectrometry at KRISS. The error bars indicate standard uncertainty for each measurement. The horizontal grid is drawn at intervals of $10^{-6}$ in the average molar mass.

of the molar mass measurement, excluding the effect of the use of the common isotope reference gas. The three absolute values of $M_{\mathrm{Ar}}$ are in mutual agreement, within the combined uncertainty of the measurements.

In summary, figure 8 indicates that three measurements of the *absolute* values of $M_{\mathrm{Ar}}$ of the gas NIM Argon-01 are in mutual agreement. One measurement achieved the uncertainty $u_{\mathrm{r}}(M_{\mathrm{Ar}}) = 0.93 \times 10^{-6}$ by using AGT at NIM and relying on an argon-isotope reference standard prepared for NIST from isotopically-enriched $^{40}$Ar. Two of these measurements achieved the uncertainty $u_{\mathrm{r}}(M_{\mathrm{Ar}}) = 0.60 \times 10^{-6}$ by using mass spectrometry at KRISS and relying on KRISS's gravimetrically-prepared, argon isotope standard. The agreement among independent measurements using independent techniques and independent standards gives us confidence that both techniques are well-understood and their results are reliable within the claimed uncertainties.

## 4. Discussion

### 4.1. Mass fractionation

The mass fractionation among different isotopes is widely used to verify the consistency of the multiple isotope analyses and to compare analyses among laboratories. It is generally assumed that in the course of the purification procedure of atmospheric argon for the production of high-purity commercial argon the fractional changes of $R_{38/36}$ and $R_{40/36}$ are inversely proportional to the square root of the mass of its particles; $(\Delta R_{38/36}/R_{38/36}) \propto \sqrt{M_{36}/M_{38}}$ and $(\Delta R_{40/36}/R_{40/36}) \propto \sqrt{M_{36}/M_{40}}$ with a common proportionality constant. Under this assumption, the changes in $R_{38/36}$ and $R_{40/36}$ are not independent; they occur only along a specific line on the $R_{38/36} - R_{40/36}$ plane.

The circles in figure 9 illustrate the isotope abundance ratios of $R_{40/36}$ plotted against $R_{38/36}$ for the data collected from April to December 2014 by the KRISS mass spectrometer. All of the measurements in this work and additional measurements for the stability check of the spectrometer are included. To a large extent, the collected data is consistent with the natural mass fractionation line shown as a dashed sloping line. The

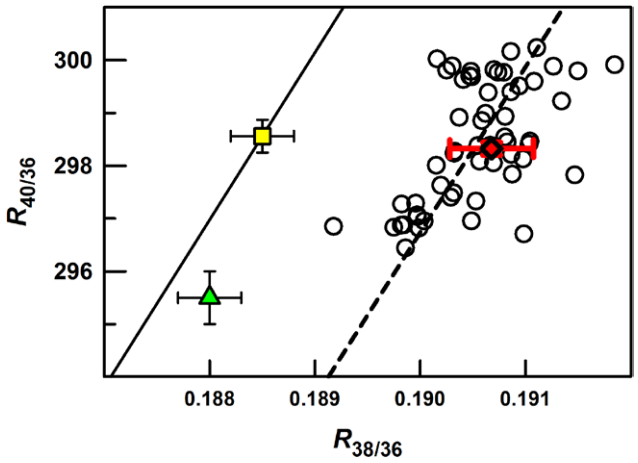


**Figure 9.** Distribution of the isotope measurements in this work (circles) and the fractionation line (dashed) that represents them. The triangle is Nier's results for atmospheric argon [16]. The square and the solid fractionation line through it that represents the 2006 results for atmospheric argon by Lee *et al* [11].

RMS of the horizontal distance $\Delta R_{38/36}$ of each data from the fractionation line is 0.000 42, which corresponds to 0.07 ppm of $M_{\mathrm{Ar}}$. The thick diamond and the uncertainty bars attached to it are the isotope abundance ratios of the sample G-LNE1-d and the short-term repeatability of the mass spectrometer measurement.

In figure 9, we also indicate the isotope ratios of atmospheric argon from Nier in 1950 (triangle) [16] and Lee *et al* in 2006 (square) [11] and their claimed uncertainties. The fractionation line based on the Lee *et al* measurement is drawn as a solid sloping line. The fractionation line that represents the data in the present work is on the side of higher $R_{38/36}$ ratio than that of the two other measurements on atmospheric argon. The uncorrected ion current ratios measured at SUERC for various argon samples are consistent with the fractionation line of Lee *et al* [17].

This work and the work of Lee *et al* share the same isotope reference gases; however, Lee *et al* measured the isotope abundance ratios $R_{38/36}$ using a dynamic isotope ratio mass spectrometer Finnigan MAT 252 at University of California San Diego [11]. In our experience, the mass spectrometer MAT 271 at KRISS normally results higher values of $R_{38/36}$ than measured elsewhere, and we do not understand the reason for this offset. We speculate that the dominant signal from $^{40}$Ar affects the measurement of $^{38}$Ar isotope in the KRISS mass spectrometer. One way to avoid this problem would be to measure the mass discrimination $f_{\mathrm{MD}}$ for $R_{38/36}$ separately from that for $R_{40/36}$. However, in the KRISS isotope reference gases $^{38}$Ar is not included as a controlled ingredient by a gravimetric mixing, but it is included only as isotopic 'impurity.' Also, in the high-purity near-atmospheric argon gas the fractional abundance of $^{38}$Ar is only ~0.000 636. Therefore, this alternative method would result much higher uncertainty $u(R_{38/36})$ than $u(R_{38/36})$ in the present work.

In this work, we did not attempt to correct for the possible, incompletely-understood, offset in $R_{38/36}$. We note that if the shift of the fractionation line is solely due to an offset in $R_{38/36}$ and not at all due to $R_{40/36}$, then we may have to adjust the

measured data $R_{38/36}$ by −0.0021 to make it consistent with the fractionation line of Lee *et al*. This corresponds to the fractional increase of 0.35 ppm in $M_{Ar}$. If this possible offset in our measurement of $R_{38/36}$ is taken into account, the uncertainty in the absolute values of $M_{Ar}$ determined using the KRISS mass spectrometer needs to be increased from $u_r(M_{Ar}) = 0.60$ ppm to $u_r(M_{Ar}) = 0.70$ ppm.

### 4.2. Absolute value of the $M_{Ar}$ measurements at KRISS

The absolute values of $M_{Ar}$ determined by the KRISS mass spectrometer rely on the gravimetrically mixed isotope reference R3 that was used during the analysis of atmospheric argon conducted at KRISS in 2006. Therefore, we assumed that the isotope ratio $R_{40/36}$ of this reference gas did not change during the 8 years since its preparation. In 2006, Lee *et al* also prepared the isotopic reference gas R2 by gravimetric mixing high purity argon (whose isotope abundance ratios were similar to those of atmospheric argon) with argon enriched in the isotope $^{36}$Ar. For R2, $R_{40/36} = 39.596$. In December 2014, after measurements of argon samples in the present work, the mass discrimination $f_{MD}$ of the KRISS mass spectrometer was measured using R3 and R2. The results of the measurement were −0.001 69 and −0.001 71, respectively, thus nearly identical. The effect of this small difference on $M_{Ar}$ of near-atmospheric argon is only 0.028 ppm. This means that either (1) the isotope ratios $R_{40/36}$ for the two reference gases have been unchanged since their preparation, or (2) they have changed by the same fraction. Alternative (2) is highly unlikely because R3 and R2 have very different isotope ratios, and because they have been stored in cylinders with different volumes and pressures. (When they were prepared, R3 was in a 6 L cylinder with pressure 0.34 MPa and R2 was a 0.075 L cylinder with pressure 8 MPa.) Furthermore, R2 has been used far less frequently than R3. The integrity of R3 and R2 is additionally supported by the agreement of KRISS' value of $M_{Ar}$ with NIM's value of $M_{Ar}$ obtained by the NIM frequency-ratio measurement with NIST Ar-40 (figure 8, and section 3.3).

We note that KRISS' uncertainty $u_r(M_{Ar}) = 0.60$ ppm (or 0.70 ppm after possible offset in $R_{38/36}$ discussed in section 4.1 is treated as uncertainty.) is realistic one (i.e. no under- or over-estimation). The difference between KRISS' two values of $M_{Ar}$ determined for two cylinders of NIM Argon-01 from the same source was 0.67 ppm (figure 8). The two estimations of the offset of the KRISS $M_{Ar}$ measurement from the SUERC measurement by the indirect comparison (through the sample C-NPL, section 3.2.1) and direct comparison (through the sample NPL EE/Iso5, section 3.2.2) was 0.88 ppm. These differences are larger than the short-term repeatability and comparable to $u_r(M_{Ar})$. This was expected because the maintenance of the mass spectrometer at the end of October 2014 removed the short-term correlations in the measurements as discussed in section 3.2.2. We emphasize that these estimates are one standard uncertainty of $M_{Ar}$ corresponding to 68% confidence limit.

### 4.3. Comments on IRMM and SUERC $M_{Ar}$ measurements

From figure 6, it is clear that the some of the mass spectrometer measurements at KRISS and IRMM are mutually inconsistent. Out of five samples that have been compared in the present work (four direct comparisons and one indirect comparison) three showed clear discrepancy that is much larger than the combined uncertainty of the two measurements. On the other hand, our measurements on 9 argon samples from several laboratories show that the isotope measurement at KRISS are self-consistent and consistently correlated with the resonance frequency measurements at LNE which use completely different physical principles. Therefore, we think that the inconsistency is due to the IRMM measurements.

However, for existing IRMM results that were used for the determination of $k_B$ in NPL-10 and LNE-11, the differences in $M_{Ar}$ between IRMM and KRISS were small. The fractional offsets of the IRMM $M_{Ar}$ measurements were +0.04 ppm (NPL AA/1; although isotope ratios were very different.), +0.27 ppm (NPL BB/2) and +0.88 ppm (through indirect comparison in section 3.1) with respect to the KRISS measurements. The uncertainty of KRISS value of $M_{Ar}$ or NIM acoustic comparison that supported the absolute values of KRISS $M_{Ar}$ is not much smaller than these offsets for the three samples. The evidence provided in the present work is not convincing enough for us to argue that the IRMM measurements of $M_{Ar}$ used in NPL-10 or LNE-11 should be replaced with the corresponding KRISS value of $M_{Ar}$. Perhaps decisive evidence resolving the discrepancies in $M_{Ar}$ could be obtained by conducting acoustic frequency-ratio measurements using the samples NPL CC/3 and/or NPL DD/4 because the two mass spectrometer analyses differed by more than 3 ppm for these samples. We are planning another approach to resolving the discrepancies, namely refining both (1) the mass spectrometer measurements and (2) the acoustic comparisons. To achieve (1) we will prepare new argon isotope reference mixtures using the gravimetric method. By increasing the amount of argon isotopes by a factor of 10 compared to the previous reference gases, we can significantly reduce the uncertainty from the isotope reference. To achieve (2) we are planning to conduct more accurate measurements of acoustic frequency ratio of the working argon gas and isotope $^{40}$Ar using the AGT at LNE. We recall that the acoustic resonance frequencies of commercial argon and $^{40}$Ar differ by approximately 185 ppm. It would be reckless to assume that the correction to the AGT frequencies from the shell's recoil is constant over this comparatively wide frequency range. Therefore the frequency ratio measurements will be conducted at two or more working pressures.

The offset of the SUERC $M_{Ar}$ measurement from the KRISS measurement is also concerning. Both measurements rely on the same isotope reference gas prepared at KRISS. Several possibilities of error in the measurement of $M_{Ar}$ for original NPL-13 $k_B$, as well as $M_{Ar}$ of atmospheric argon are discussed elsewhere in this issue [18]. However, in this paper we emphasize that atmospheric argon was used as a transfer standard in the SUERC measurement. In contrast, our measurements are

directly linked to the R3 reference gas and confirmed by the R2 reference and NIM acoustic comparison. When the isotopic composition of atmospheric argon was re-determined in 2006, the geochemistry and geochronology communities did not foresee the use of $R_{40/36}$ and $R_{38/36}$ of atmospheric argon as standards to determine absolute value of $M_{Ar}$ with uncertainties of 1 ppm or smaller. To achieve such small uncertainties, it is necessary to prove the global constancy of $M_{Ar}$ of atmospheric argon and to reexamine the purification and handling of atmospheric argon.

## Acknowledgments

The authors thank Deulae Min for the measurement of the argon isotope reference at KRISS and Michael de Podesta for providing argon samples and helpful discussion on the isotope analysis. The work at KRISS was supported by Grant 14011034 from the Korea Research Institute of Standards and Science under the project 'Establishment of National Physical Measurement Standards and Improvements of Calibration/Measurement Capability.'

## References

[1] Comptes Rendus de la 25e CGMP 2014 On the future revision of the International System of Units, the SI p 2 (www.bipm.org/utils/common/pdf/CGPM/CGPM25.pdf#page = 2)
[2] White D R and Fischer J (ed) 2015 *Metrologia* **52** (special issue)
[3] Mohr P J, Taylor B N and Newell D B 2012 CODATA recommended values of the fundamental physical constants: 2010 *Rev. Mod. Phys.* **84** 1527–605
[4] Moldover M R, Gavioso R M. Mehl J B, Pitre L, de Podesta M and Zhang J T 2014 Acoustic gas thermometry *Metrologia* **51** R1–19
[5] Mohr P J, Newell D B and Taylor B N 2014 CODATA recommended values of the fundamental physical constants (http://pml.nist.gov/constants)
[6] Moldover M R, Trusler J P M, Edwards T J, Mehl J B and Davis R S 1988 Measurement of the universal gas constant *r* using a spherical acoustic resonator *J. Res. Natl Bur. Stand.* **93** 85–144
[7] Sutton G, Underwood R, Pitre L, de Podesta M and Valkiers S 2010 Acoustic resonator experiments at the triple point of water: first results for the Boltzmann constant and remaining challenges *Int. J. Thermophys.* **31** 1310–46
[8] Pitre L, Sparasci F, Truong D, Guillou A, Risegari L and Himbert M 2011 Measurement of the Boltzmann constant $k_B$ using a quasi-spherical acoustic resonator *Int. J. Thermophys.* **32** 1825–86
[9] de Podesta M, Underwood R, Sutton G, Morantz P, Harris P, Mark D F, Stuart F M, Vargha G and Machin G 2013 A low-uncertainty measurement of the Boltzmann constant *Metrologia* **50** 354–76
[10] Lin H, Feng X J, Gillis K A, Moldover M R, Zhang Z T, Sun J P and Duan Y Y 2013 Improved determination of the Boltzmann constant using a single, fixed-length cylindrical cavity *Metrologia* **50** 417–32
[11] Lee J-Y, Marti K, Severinghaus J P, Kawamura K, Yoo H-S, Lee J B and Kim J S 2006 A redetermination of the isotopic abundance of atmospheric Ar *Geochim. Cosmochim. Acta* **70** 4507–12
[12] de Laeter J R, Böhlke J K, Bièvre P D, Hidaka H, Peiser H S, Rosman K J R and Taylor P D P 2003 Atomic weights of the elements. Review 2000 (IUPAC technical report) *Pure Appl. Chem.* **75** 683–800
[13] Valkiers S, Vendelbo D, Berglund M and de Podesta M 2010 Preparation of argon Primary Measurement Standards for the calibration of ion current ratios measured in argon *Int. J. Mass Spectrom.* **291** 41–7
[14] Zhang J T, Lin H, Feng X J, Sun J P, Gillis K A, Moldover M R and Duan Y Y 2011 Progress toward redetermining the Boltzmann constant with a fixed-path-length cylindrical resonator *Int. J. Thermophys.* **32** 1297–329
[15] Feng X J, Lin H, Gillis K A, Moldover M R and Zhang J T 2015 Test of a virtual cylindrical acoustic resonator for determining the Boltzmann constant *Metrologia* **52** S343–52
[16] Nier A 1950 A redetermination of the relative abundances of the isotopes of carbon, nitrogen, oxygen, argon, and potassium *Phys. Rev.* **77** 789–93
[17] Mark D F, Stuart F M and de Podesta M 2011 New high-precision measurements of the isotopic composition of atmospheric argon *Geochim. Cosmochim. Acta* **75** 7494–501
[18] de Podesta M, Yang I, Mark D F, Underwood R, Sutton G and Machin G 2015 Correction of NPL-2013 estimate of the Boltzmann constant for argon isotopic composition and thermal conductivity *Metrologia* **52** S353–63